Effects of Non-Covalent Self-Association on the Subcutaneous Absorption of a Therapeutic Peptide

Dean K. Clodfelter,[1] Allen H. Pekar,[1] Dawn M. Rebhun,[1] Kevin A. Destrampe,[1] Henry A. Havel,[1] Sharon R. Myers,[2] and Mark L. Brader[1,3]

Received July 31, 1997; accepted November 7, 1997

Purpose. To utilize an acylated peptide as a model system to investigate the relationships among solution peptide conformation, non-covalent self-association, subcutaneous absorption and bioavailability under pharmaceutically relevant solution formulation conditions.

Methods. CD spectroscopy, FTIR spectroscopy, equilibrium sedimentation, dynamic light scattering, and size exclusion chromatography were employed to characterize the effects of octanoylation on conformation and self-association of the 31 amino acid peptide derivative des-amino-histidine(7) arginine(26) human glucagon-like peptide (7-37)-OH (IP(7)R(26)GLP-1). Hyperglycemic clamp studies were performed to compare the bioavailability, pharmacokinetics, and pharmacodynamics of solution formulations of oct-IP(7)R(26)GLP-1 administered subcutaneously to normal dogs.

Results. Octanoylation of IP(7)R(26)GLP-1 was shown to confer the propensity for a major solvent-induced conformational transition with an accompanying solvent- and temperature-dependent self-association behavior. Formulations were characterized that give rise to remarkably different pharmacodynamics and pharmacokinetics that correlate with distinct peptide conformational and self-association states. These states correspond to: (i) a minimally associated α-helical form (apparent molecular weight = 14 kDa), (ii) a highly associated, predominantly β-sheet form (effective molecular diameter 20 nm), and (iii) an unusually large, micelle-like soluble β-sheet aggregate (effective molecular diameter 50 nm).

Conclusions. Bioavailability and pharmacokinetics of a self-associating peptide can be influenced by aggregate size and the ease of disruption of the non-covalent intermolecular interactions at the subcutaneous site. Hydrophobic aggregation mediated by seemingly innocuous solution formulation conditions can have a dramatic effect on the subcutaneous bioavailability and pharmacokinetics of a therapeutic peptide and in the extreme, can totally preclude its absorption. A size exclusion chromatographic method is identified that distinguishes subcutaneously bioavailable aggregated oct-IP(7)R(26)GLP-1 from non-bioavailable aggregated oct-IP(7)R(26)GLP-1.

KEY WORDS: peptide; aggregation; subcutaneous absorption; glucagon-like peptide-1.

[1] Biopharmaceutical Development, Lilly Research Laboratories, Eli Lilly and Company, Indianapolis, Indiana 46285.

[2] Diabetes Research, Lilly Research Laboratories, Eli Lilly and Company, Indianapolis, Indiana 46285.

[3] To whom correspondence should be addressed. (E-mail: brader_m_1@lilly.com)

ABBREVIATIONS: Glucagon-like peptide-1(7-37)-OH (GLP-1); imidazopropionyl(7) arginine(26) lysine(34)-human glucagon-like peptide-1 (IP(7)R(26)GLP-1); imidazopropionyl(7) arginine(26) N^{ε}-octanoyl-lysine(34)-human glucagon-like peptide-1 (oct-IP(7)R(26) GLP-1); circular dichroism, CD; size exclusion chromatography, SEC; Fourier transform infrared, FTIR; phosphate buffered saline, PBS.

INTRODUCTION

The efficacy of subcutaneously administered therapeutic proteins and peptides is critically dependent upon the absorption and subsequent delivery of the biologically active form of the drug to the site of action. The task of the formulation scientist includes conferring the appropriate shelf-life and in-use stability as well as stabilizing the molecule in a form that facilitates optimal bioavailability and biopotency. The formulation design may also play the principal role in mediating drug absorption thus providing a means to tailor appropriate pharmacokinetics for the drug. Currently, most biopharmaceuticals are administered via subcutaneous injection or intravenous infusion. While the importance of chemical and physical stability are obvious, the potential pharmacological consequences of non-covalent solution structural phenomena such as alternative molecular conformations and/or self-association may be a poorly appreciated but critical aspect of the overall therapeutic success of the drug. This is particularly relevant to discovery and early stage drug development where a large-scale screening strategy or an emphasis on speed-to-first-efficacy-dose may preclude a detailed solution characterization of the molecule prior to dosing (1). The non-covalent aggregation of protein pharmaceuticals is a well recognized problem that has been studied largely in the context of insoluble forms, including precipitates, fibrils, and gels (2,3). These insoluble products have been attributed to the formation of partially unfolded intermediates with an exposed hydrophobic region that drives the aggregation towards the pharmaceutically undesirable form (2–4). Previous studies of this mechanism have been performed by introducing a denaturant to generate the partially unfolded intermediate (4,5). By studying an acylated peptide we have effectively introduced an artificial hydrophobic region to the surface of the peptide in the absence of a denaturant. This approach has facilitated an investigation of the relationship between hydrophobic aggregation and subcutaneous bioavailability under pharmaceutically relevant solution conditions.

Glucagon-like peptide-1(7-37)-OH (GLP-1) is a 31 amino acid hormone liberated by the proteolytic processing of the 160 amino acid precursor protein, preproglucagon. GLP-1 stimulates the secretion of insulin and thus has the ability to normalize blood glucose levels (6). Interest in GLP-1 and its analogs has intensified recently as the attractiveness of GLP-1 as a potential therapeutic agent for the treatment of type II diabetes has been recognized (6–8). The structure of the analog we have studied is shown in Figure 1 and will be abbreviated as oct-IP(7)R(26)GLP-1. This molecule exhibits three changes from the native GLP-1(7-37)-OH structure: the amino group has been removed from the His(7) residue (becoming des-amino-histidine, or imidazopropionyl and is abbreviated herein as IP), Lys(26) has been replaced by Arg, and Lys(34) has been acylated with the straight chain fatty acid octanoic acid (abbreviated as oct). The present study characterizes the effect of the octanoyl acylation on the structure, conformation and self-association of this GLP-1 analog and demonstrates that these properties are highly solvent dependent. This molecule thus affords an opportunity to investigate the relationships among peptide secondary structure, non-covalent molecular association, subcutaneous bioavailability and the pharmacodynamics

0724-8741/98/0200-0254$15.00/0

of a single therapeutic peptide formulated under different, pharmaceutically typical solution conditions. Of additional significance to this study is the fact that the acylation of proteins *in vivo* is a recently recognized covalent modification involved in intracellular signaling pathways (9). The way in which the acylation mediates these processes is poorly understood. The IP(7)R(26) GLP-1 moiety thus represents a useful model system to investigate the effects of acylation on peptide conformational and associative behavior.

MATERIALS AND METHODS

Materials

Oct-IP(7)R(26)GLP-1 and IP(7)R(26)GLP-1 were provided by Eli Lilly and Company as highly purified lyophilized powders. All other chemicals were of analytical reagent grade. Dulbecco's phosphate buffered saline without Ca and Mg (PBS) was obtained from ICN Biomedical Inc. Solution concentrations of oct-IP(7)R(26)GLP-1 and IP(7)R(26)GLP-1 were calculated based on the respective extinction coefficients of 1.95 $(mg/ml)^{-1} \cdot cm^{-1}$ and 2.01 $(mg/ml)^{-1} \cdot cm^{-1}$ at 279 nm.

Size Exclusion Chromatography

Based on criteria of selectivity and resolution, a 25 cm × 9.4 mm Zorbax GF-250 special column was chosen for the present studies with a mobile phase comprising 14 mM sodium phosphate dibasic adjusted to pH 7.4 with 85% phosphoric acid. The flow rate was 1 ml/min and the injection volume was 50 µl of a 1 mg/ml solution. The eluent was detected using UV absorbance at 214 nm. (Detailed studies to investigate the chromatographic properties of several SEC columns under various mobile phase conditions were undertaken and will be reported elsewhere (10)).

Circular Dichroism Spectroscopy

Circular dichroism spectra were recorded using an AVIV Model 62A DS spectrometer calibrated with (1S)-(+)-10-camphorsulfonic acid. Circular dichroism is reported as mean residue elipticity, $[\theta]_\lambda$, having units of degrees $\cdot cm^2 \cdot dmol^{-1}$. Secondary structural analyses were performed using the program CONTIN (11–12).

Analytical Ultracentrifugation

Sedimentation equilibrium experiments were carried out at 4 °C in a Beckman XLA analytical ultracentrifuge using absorbance optics. Cells with quartz windows and either 3 mm or 12 mm centerpieces were used. The apparent weight-average molecular weights, $M_{w,app}$, were calculated from equation (1).

$$M_{w,app} = \left(RT/\left((1 - v\rho)\omega^2 rC\right) \cdot dC/dr \right. \quad (1)$$

where R is the gas constant, **T** is temperature, *v* is the partial specific volume, ρ is the solvent density, r is radius, ω is the angular velocity and C is the total protein concentration in mg/ml. A partial specific volume of 0.726 ml/gram was calculated from the amino acid composition (13). It was assumed that the addition of the acyl group did not change the value of *v*. The solvent density was measured using a Paar DMA48 densitometer. Data analyses to model the self-association and determine equilibrium constants (14) were carried out using the program NONLIN, available through the National Analytical Ultracentrifuge Facility at the University of Connecticut. NONLIN gives values of equilibrium constants $k_{1,n}$ on (a mg/ml concentration scale) which refer to the reversible formation of an n-mer from n monomeric units, as described by equation (2). (Thus the tetramer constant $k_{1,4}$ corresponds to the reaction of four monomers to give a tetramer; $k_{1,8}$ corresponds to the reaction of eight monomers to give an octamer; $k_{4,8}$ corresponds to the reaction of two tetramers to give an octamer). The corresponding molar equilibrium constant $K_{1,n}$ is given by equation (3).

$$k_{1,n} = [n - mer]/[monomer]^n \quad (2)$$

$$K_{1,n} = k_{1,n} \cdot (\text{monomer molecular weight})^{n-1}/n \quad (3)$$

Infrared Spectroscopy

Infrared spectra were recorded on a Nicolet Magna 750 Fourier transform infrared spectrophotometer equipped with a Nicolet Nic-Plan infrared microscope. Data were acquired for 128 scans at 4 cm^{-1}. Data acquisition and second derivative analysis were performed with Omnic 3.1 software.

Dynamic Light Scattering

Measurements were performed using a Brookhaven Instruments 9000 autocorrelator and goniometer. All measurements were made with a 400 µm pinhole at a 90° scattering angle using a Lexel Model 3500 argon ion laser set at 488 nm as the scattering source. Sample temperature was maintained at 25°C or 5°C by a Neslab RTE-110 temperature bath. Brookhaven Instruments software was used to calculate the diffusion coefficients of the scattering species from the measured autocorrelation function using the method of cumulants. Diffusion coefficients were converted to mean diameters using the Stokes-Einstein relationship. Values for solution viscosities and refractive indices were assumed to be equal to those of pure water.

In Vivo Testing

Study Design and Animals

GLP-1 is an incretin peptide hormone that stimulates insulin secretion from the β-cell in a glucose dependent manner (6). Hyperglycemic clamp experiments (150 mg/dl) were conducted using chronically cannulated, overnight-fasted, conscious male and female beagle dogs weighing 8–15 kg. Pharmacodynamics were evaluated from the plasma insulin data and pharmacokinetics were determined from blood drug levels. The insulin change and drug level areas under the curve were calculated using the trapezoidal rule. Values are reported as the mean ± the standard error of the mean. Prior to initiation of the study the animals were judged to be healthy by physical examination and laboratory tests. Research adhered to the Principles of Laboratory Animal Care of the NIH.

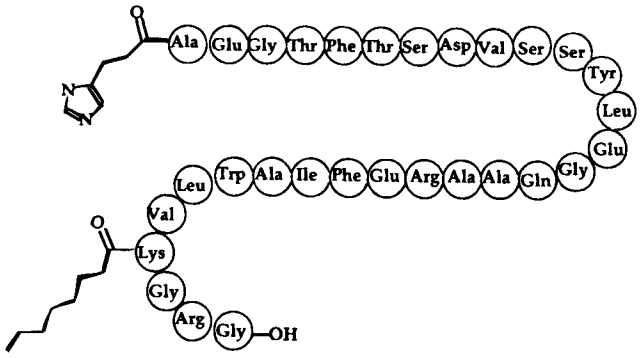

Fig. 1. The structure of imidazopropionyl(7) arginine(26) N^{ε}-octanoyl-lysine(34)-human glucagon-like peptide-1(7-37)-OH (oct-IP(7)R(26) GLP-1).

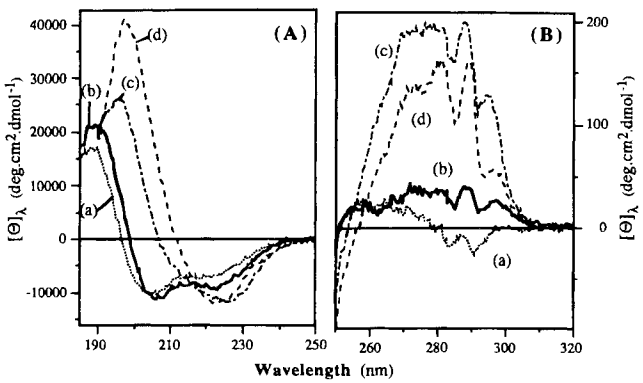

Fig. 2. Panel A: Far-UV CD spectra of IP(7)R(26)GLP-1 (a) and oct-IP(7)R(26)GLP-1 (b) prepared and recorded at 5 °C in 5 mM phosphate buffer, pH 7.5. Oct-IP(7)R(26)GLP-1 prepared and recorded at 5 °C (c) and 22 °C (d) in PBS, pH 7.5. Spectra (a) and (b) were recorded on 0.1 mg/ml and 0.02 mg/ml solutions, respectively. IP(7)R(26)GLP-1 and oct-IP(7)R(26)GLP-1 are monomeric under these conditions. Spectra (c) and (d) were recorded on 0.5 mg/ml solutions. Only minor differences in the CD spectrum of oct-IP(7)R(26) GLP-1 in PBS were apparent over the concentration range 0.1–0.5 mg/ml. Panel B: Near-UV CD spectra of IP(7)R(26)GLP-1 (a) and oct-IP(7)R(26)GLP-1 (b) prepared and recorded at 5 °C in 5 mM phosphate buffer, pH 7.5. Oct-IP(7)R(26)GLP-1 prepared and recorded at 5 °C (c) and 22 °C (d) in PBS, pH 7.5. Spectra were recorded on 0.5 mg/ml solutions.

Formulation Preparation and Administration

Formulations were injected subcutaneously into the dorsal aspect of the neck at a dose of 3 nmol/kg. Four formulations stabilizing distinct conformational and self-association states (*vide infra*) of oct-IP(7)R(26)GLP-1 were evaluated. These formulations were prepared by dissolving lyophilized oct-IP(7)R(26)GLP-1 under the following conditions: (i) 5 mM phosphate buffer, pH = 7.5 prepared at room temperature immediately prior to administration ($M_{w,app}$ approximately 14 kDa by equilibrium sedimentation) (ii) PBS, pH = 7.5 prepared at room temperature immediately prior to administration (quadratic diameter approximately 10 nm by dynamic light scattering at time of dosing) (iii) PBS, pH = 7.5 prepared and stored at 5 °C for 24 hours prior to dosing (quadratic diameter approximately 20 nm by dynamic light scattering at time of dosing), and (iv) PBS, pH = 7.5 prepared and stored at room temperature for 24 hours prior to dosing (quadratic diameter approximately 50 nm by dynamic light scattering at time of dosing).

RESULTS

Circular Dichroism Studies

The far-UV circular dichroism (CD) spectra of IP(7)R(26) GLP-1 and oct-IP(7)R(26)GLP-1 recorded under monomeric conditions in 5 mM phosphate buffer pH 7.5 are presented in Figure 2A (a) and (b) respectively. These spectra show that octanoylation causes a slight perturbation in the far-UV CD of the IP(7)R(26)GLP-1 peptide (Table I). Figure 2A (a) and (b) appear very similar to that reported for native GLP-1 (15) and were found to exhibit analogous concentration dependencies (an intensification with increasing concentration). A comparison of the CD characteristics of each molecule in 5 mM phosphate buffer pH 7.5 and in PBS showed that the IP(7)R(26) GLP-1 molecule possesses closely similar CD spectra in these two solvents, whereas the octanoylated peptide exhibits dramatically different CD spectra. The CD spectrum of Figure 2A (c) corresponds to an oct-IP(7)R(26)GLP-1 solution prepared in PBS at 5 °C. Comparison of this spectrum with Figure 2A (b) shows that a major conformational rearrangement has occurred. The CD spectrum of Figure 2A (d) corresponds to an oct-IP(7)R (26)GLP-1 solution in PBS prepared and recorded at 22 °C. The data of Table I show that under these solution conditions, an almost complete loss of α-helical structure has occurred.

The corresponding near-UV CD spectra are presented in Figure 2B. These data show that under the higher ionic strength conditions (PBS), oct-IP(7)R(26)GLP-1 is characterized by relatively intense CD features with positive maxima in the range 265–295 nm. These results show that the changes in secondary structure evident from Figure 2A are accompanied by major changes in the chromophoric environments of the aromatic residues.

Table I. Secondary Structural Analyses of the CD Spectra of Figure 2A

Peptide	Solvent	Temp./°C	%α-helix	%β-sheet	%remainder
IP(7)R(26)GLP-1	5 mM PB	5	16	40	43
oct-IP(7)R(26)GLP-1	5 mM PB	5	28	31	42
oct-IP(7)R(26)GLP-1	PBS	5	23	16	61
oct-IP(7)R(26)GLP-1	PBS	22	2	36	62

Note: Analyses were performed on 190–240 nm data using the program CONTIN (11,12). PB refers to phosphate buffer pH 7.5 and PBS refers to 10 mM phosphate buffered saline pH 7.5.

Equilibrium Sedimentation Studies

Detailed analytical ultracentrifugation experiments were performed on IP(7)R(26)GLP-1 and oct-IP(7)R(26)GLP-1 under low ionic strength conditions. In 5 mM phosphate buffer pH 7.5 at 4 °C, the non-acylated compound reached equilibrium in about 25 hours. For the acylated derivative, it was noted that a very slight loss of material occurred with time, possibly due to the slow formation of a small fraction of highly aggregated species. On the assumption that the acylated molecule was close to equilibrium, the apparent weight average molecular weights were calculated and plotted against concentration (Figure 3). Each curve was constructed using data from three cells having different loading concentrations. Overlap of these data was good for each molecule, consistent with self-association. Since native GLP-1(7-37) has been reported to self-associate to tetramers (16), an ideal monomer-tetramer-octamer self-association model was chosen. A good fit of concentration versus radius was achieved with this model for all three cells for IP(7)R(26)GLP-1 and is shown in Figure 3. For the acylated derivative, the monomer-tetramer-octamer model fit the data well in the lower concentration region but not at higher concentrations. However, by including a non-ideality term in the modeling, it was possible to achieve a good fit of these data to a monomer-tetramer-octamer association mechanism. The molar equilibrium constants obtained from the curve fit to the IP(7)R(26)GLP-1 data of Figure 3 were $K_{1,4} = 6.44 \times 10^{11}$, $K_{1,8} = 8.18 \times 10^{27}$ and $K_{4,8} = 1.97 \times 10^{4}$, where $K_{1,4}$ and $K_{1,8}$ correspond respectively to the formation of tetramers and octamers from monomers and $K_{4,8}$ corresponds to the formation of octamers from tetramers. For oct-IP(7)R(26)GLP-1 the values were $K_{1,4} = 7.29 \times 10^{14}$, $K_{1,8} = 4.00 \times 10^{33}$ and $K_{4,8} = 7.53 \times 10^{3}$. These models generated good fits to the experimental data (Figure 3), although we note that they may not necessarily represent unique fits. The larger value of $K_{1,4}$ for the acylated derivative is consistent with the greater concentration dependence of weight average molecular weight over the 0–0.5 mg/ml concentration range. However, the subsequent formation of octamers from tetramers is somewhat smaller for the acylated compound than for the non-acylated compound.

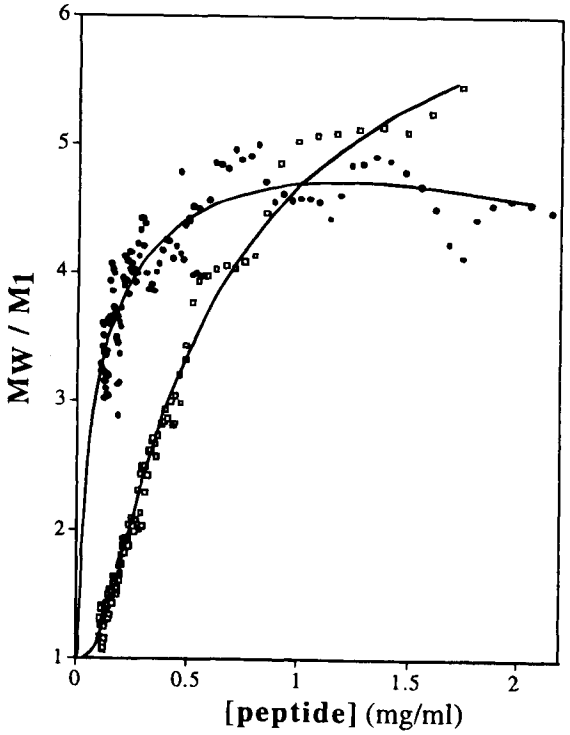

Fig. 3. Equilibrium sedimentation data for IP(7)R(26)GLP-1 (open symbols) and oct-IP(7)R(26)GLP-1 (solid symbols) in 5 mM phosphate buffer pH = 7.5, 4 °C. The solid curves were calculated for a monomer-tetramer-octamer self-association mechanism using the program NONLIN. M_w/M_1 represents the weight average molecular weight obtained from ultracentrifugation divided by the molecular weight of monomer.

Dynamic Light Scattering

In view of the extreme degree of aggregation of oct-IP(7)R(26)GLP-1 in PBS, dynamic light scattering was selected as the most appropriate technique to characterize self-association under these solution conditions. The time-dependence of the aggregation of oct-IP(7)R(26)GLP-1 in PBS at 25 °C and 5 °C as monitored by dynamic light scattering is shown in Figure 4 (a) and (b) respectively. These data show that upon initial reconstitution of the lyophilized powder in PBS at 5 °C, the quadratic diameter is approximately 10 nm. This value increases to about 20 nm over a period of 24 hours. In contrast, for the reconstitution in PBS at 25 °C, the initial quadratic diameter is approximately 20 nm. This value increases to about 50 nm over a period of 24 hours.

Size Exclusion Chromatography

The solvent-dependent CD spectral characteristics of oct-IP(7)R(26)GLP-1 were found to be accompanied by a distinctive size exclusion chromatographic (SEC) signature. The SEC

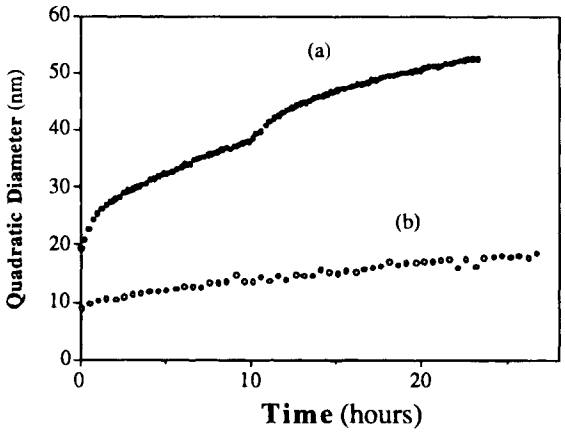

Fig. 4. Dynamic light scattering data for a 0.5 mg/ml solution of oct-IP(7)R(26)GLP-1 formulated in PBS at 25 °C (a) and 5 °C (b). These data show the time dependence of the aggregation of oct-IP(7)R(26)GLP-1 under these solution conditions. The aggregation states shown by dataset (a) at t = 0 and t = 24 hours correspond to those of the samples administered in the dog studies of Figure 7 A and B (b) and Figure 7 C and D (c), respectively. The aggregation state shown by dataset (b) at t = 24 hours corresponds to that of the PBS sample administered in the dog study of Figure 7 C and D (b).

profiles of IP(7)R(26)GLP-1 and oct-IP(7)R(26)GLP-1 prepared in 5 mM phosphate buffer pH 7.5 are presented in Figure 5 (a) and (b) respectively. SEC profiles (c) and (d) correspond to oct-IP(7)R(26)GLP-1 solutions prepared in PBS at 5 °C and 22 °C respectively, and aged at these temperatures for 24 hours prior to analysis. These data show that the SEC retention times of oct-IP(7)R(26)GLP-1 solutions prepared in 5 mM phosphate buffer at 5 °C and in PBS at 5 °C are equivalent. However, in PBS at 22 °C the SEC retention time of oct-IP(7)R(26)GLP-1 is dramatically different and indicative of a much higher apparent molecular weight. It was determined that this aggregated species could be disaggregated in solution by incorporating 30% acetonitrile into the PBS solvent. SEC analysis of this sample (Figure 5 (e)) produced an SEC retention time equal to that of Figure 5 (b). This result indicates that the species corresponding to the SEC peak in Figure 5 (d) is a hydrophobically associated soluble aggregate. The broadness of the oct-IP(7)R (26)GLP-1 peak in (b)–(e) is probably due to enhanced hydrophobic interactions between the peptide and the column packing in addition to on-column equilibria involving a range of aggregation states (17). The chromatograms of Figure 5 (b) and (c) exhibit the same retention time, however, the dynamic light scattering and equilibrium sedimentation data presented herein show that these samples correspond to different states of self-association. The difference between these two aggregation states is not evident by this SEC method, thus it is inferred that the SEC column conditions disrupt the non covalent self-association that occurs in PBS at 5 °C. In contrast, the SEC characteristics suggest a different entity in PBS at 22 °C, an interpretation in accord with the dynamic light scattering data of Figure 4 and the distinctive CD spectroscopic characteristics. Evidently, the peptide molecules are more strongly self-associated in PBS at 22 °C than under the solution conditions of Figure 5 (a)–(c). It is speculated that this aggregate corresponds to a micellar species for which the different CD and SEC characteristics in PBS at 5 °C versus 22 °C, correspond to temperatures that bracket the critical micelle temperature.

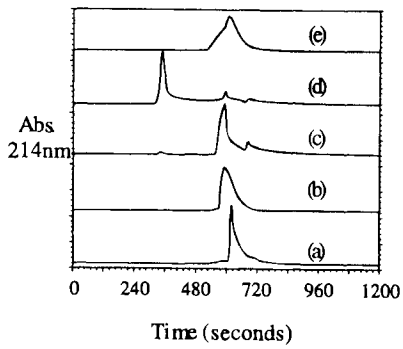

Fig. 5. Size exclusion chromatograms recorded on IP(7)R(26)GLP-1 (a) and oct-IP(7)R(26)GLP-1 (b) solutions prepared at 5 °C in 5 mM phosphate buffer, pH = 7.5. Chromatograms (c) and (d) were recorded on oct-IP(7)R(26)GLP-1 solutions prepared in PBS at 5 °C and 22 °C respectively, and aged at these temperatures for 24 hours prior to analysis. Chromatogram (e) corresponds to a solution of oct-IP(7)R(26)GLP-1 prepared in an identical manner to (d) that had 30% acetonitrile incorporated into the sample solvent immediately prior to SEC analysis. All samples were prepared at a peptide concentration of 1 mg/ml.

Infrared Spectroscopy

Infrared spectroscopy provides a convenient method to probe protein conformation and structure in the solid state. The infrared spectral profiles of the amide region of oct-IP(7)R (26)GLP-1 are presented in Figure 6. Spectrum (A) corresponds to oct-IP(7)R(26)GLP-1, lyophilized from 5 mM phosphate buffer pH 7.5. This spectrum exhibits amide I and amide II bands at 1659 cm^{-1} and 1542 cm^{-1} respectively, values consistent with an appreciable α-helical secondary structure content (18). Spectra (B) and (C) correspond to samples of oct-IP(7)R (26)GLP-1 each lyophilized from PBS, pH 7.5, that had been aged 24 hours at 5 °C and 22 °C respectively. Spectra (B) and (C) both exhibit features at 1695 cm^{-1} (shoulder) 1660 cm^{-1} (main) and 1625 cm^{-1} (shoulder), resolved in the second derivative spectra (not shown). By comparison to spectrum (A) these spectra show that a major conformational change has taken place as a result of dissolving oct-IP(7)R(26)GLP-1 in PBS prior to lyophilization. The IR spectral profiles of (B) and (C) are consistent with a significant increase in β-sheet content (18). The data of Figure 6 establish that in the solid state the oct-IP(7)R(26)GLP-1 species can adopt a secondary structure that is either predominantly α-helical or predominantly β-sheet depending upon the solution conditions from which it was lyophilized. These infrared results on the solid state are in conformity with the CD data for oct-IP(7)R(26)GLP-1 in solution.

In Vivo Testing

The data of Figure 7 compare the plasma insulin responses (A and C) and the plasma drug levels (B and D) for oct-

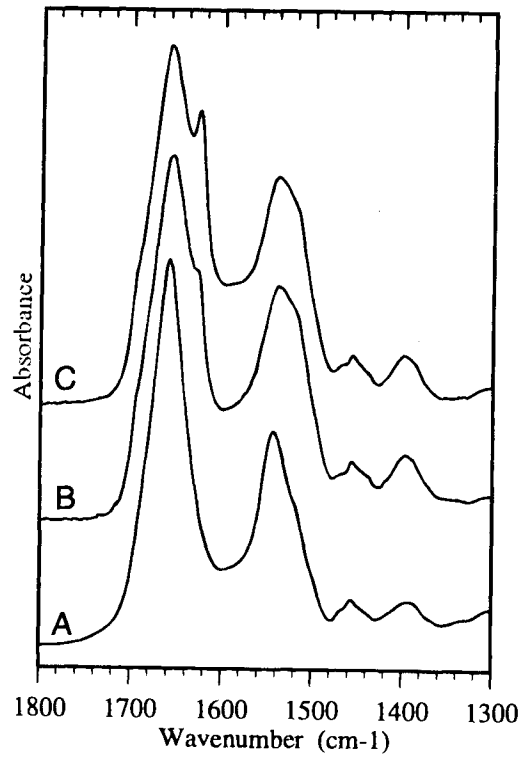

Fig. 6. FTIR spectra recorded on solid samples of oct-IP(7)R (26)GLP-1 prepared by lyophilization from the following solutions; (A) 5 mM phosphate buffer, pH 7.5, T = 5 °C (B) PBS, pH 7.5, T = 5 °C (C) PBS, pH 7.5, T = 22°C.

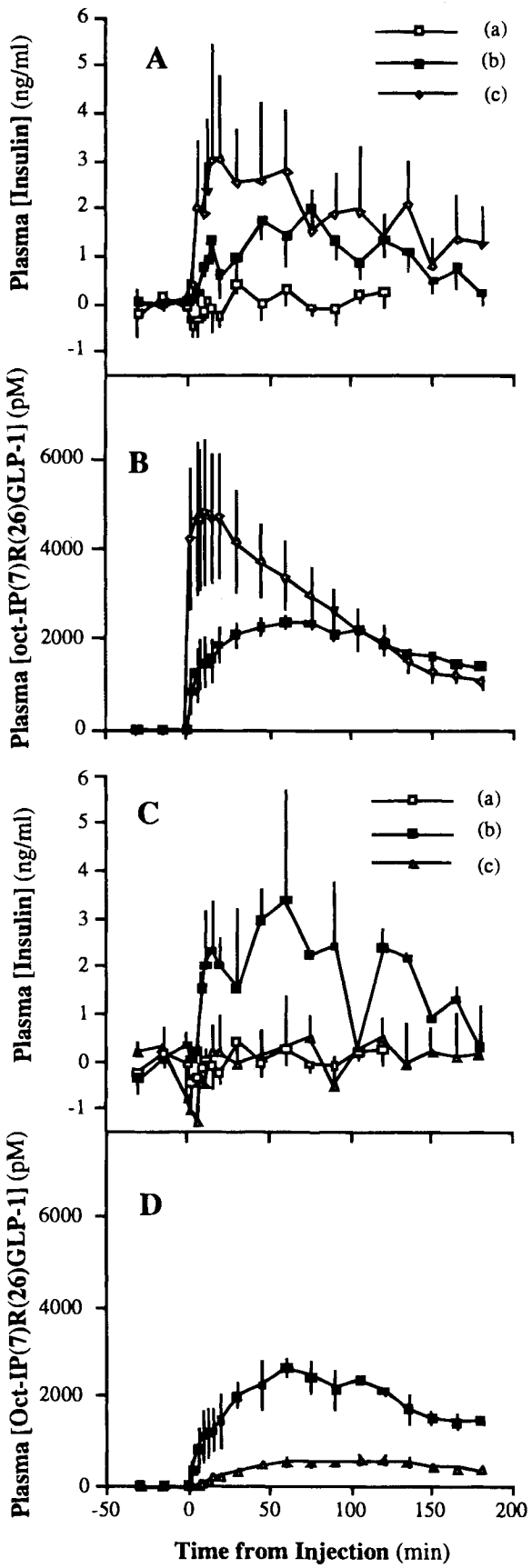

IP(7)R(26)GLP-1 administered under four different formulation conditions. The data labeled (a) correspond to a vehicle control in which PBS was administered. In Figure 7 A and B, the curves labeled (c) correspond to oct-IP(7)R(26)GLP-1 formulated in 5 mM phosphate buffer, and the curves labeled (b) correspond to oct-IP(7)R(26)GLP-1 formulated in PBS at room temperature and administered immediately upon dissolution of the lyophilized oct-IP(7)R(26)GLP-1 in these solvents. In this experiment, the quadratic diameter of the peptide in the formulation corresponding to (b) was determined by dynamic light scattering to be 20 nm (Figure 4). The apparent molecular weight of the formulation corresponding to (c) was determined by equilibrium sedimentation to be about 14 kDa. The data of Figure 7 A and B show that oct-IP(7)R(26)GLP-1 formulated in 5 mM phosphate buffer, pH 7.5 elicits a more rapid onset of action and is more rapidly absorbed from the subcutaneous site than the PBS formulation. The areas under the curves A(b) and A(c) are 190 ± 50 and 340 ± 140 ng/ml· min respectively. The areas under the curves B(b) and B(c) are 240,000 ± 20,000 and 400,000 ± 90,000 pM·min respectively. This comparison suggests that the bioavailability of oct-IP(7)R(26)GLP-1 is greater for the 5 mM phosphate buffer formulation than for the PBS formulation.

The data of Figure 7 C and D compare the plasma insulin response and the plasma drug levels for oct-IP(7)R(26)GLP-1 formulated in PBS and aged 24 hours at 5 °C (b) and at room temperature (c) prior to administration. The dynamic light scattering data of Figure 4 shows that these formulation conditions correspond to quadratic diameters of 20 nm and 50 nm for the 5 °C and room temperature formulations respectively. The data of Figure 7 C and D show that the plasma insulin response of the PBS formulation aged at room temperature is negligible and that the plasma levels of oct-IP(7)R(26)GLP-1 are dramatically reduced. The areas under the curves C(b) and C(c) are 330 ± 90 and 10 ± 100 ng/ml· min respectively.

The areas under the curves D(b) and D(c) are 250,000 ± 40,000 and 50,000 ± 10,000 pM min respectively. These data establish that the effect of aging the oct-IP(7)R(26)GLP-1 PBS formulation at room temperature has been to diminish its absorption from the subcutaneous site so severely that its pharmacodynamic effect has been totally abolished.

DISCUSSION

The biophysical studies herein identify three distinct conformational and self-association states of oct-IP(7)R(26)GLP-1

Fig. 7. Comparison of the pharmacodynamics and pharmacokinetics of oct-IP(7)R(26)GLP-1 formulated under four different solution conditions. Plasma insulin response and oct-IP(7)R(26)GLP-1 concentrations were measured in normal, overnight-fasted dogs after subcutaneous injection of 3 nmol/kg of oct-IP(7)R(26)GLP-1. Vehicle controls (n = 5) correspond to a subcutaneous injection of PBS (a). *Panels A and B:* Pharmacodynamics (A) and pharmacokinetics (B) of oct-IP(7)R(26)GLP-1 in PBS (n = 6) (b) versus 5 mM phosphate buffer pH 7.5 (n = 4) (c). The formulations were prepared at room temperature and administered immediately upon reconstitution of lyophilized peptide. *Panels C and D:* Pharmacodynamics (C) and pharmacokinetics (D) of a solution of oct-IP(7)R(26)GLP-1 prepared in PBS and stored at 5 °C, (n = 2) (b) and ambient room temperature (n = 2) (c) for 24 hours prior to administration.

that are each stabilized by different, but pharmaceutically typical solution conditions. In 5 mM phosphate buffer pH = 7.5, oct-IP(7)R(26)GLP-1 possesses significant α-helical structure and exhibits an apparent molecular weight consistent with a predominantly tetrameric self-association state. In PBS, the secondary structure is predominantly β-sheet, and the self-association state is temperature dependent. At 5 °C in PBS, oct-IP(7)R(26)GLP-1 possesses a quadratic diameter of about 20 nm, whereas at 22 °C in PBS it is 50 nm and this peptide exhibits a unique SEC retention time. The biological data herein show that, in comparison to the α-helical formulation, the highly associated β-sheet form of oct-IP(7)R(26)GLP-1 retains a high level of subcutaneous bioavailability when formulated and stored at 5 °C. Evidently, under these formulation conditions the non-covalent β-sheet-β-sheet interactions are weak enough to be disrupted by dilution within the subcutaneous space, thus facilitating drug transportation and absorption. However, these additional non-covalent interactions give rise to perturbed pharmacokinetics, presumably due to altered dissociation and absorption properties at the subcutaneous site. In addition, differences in the relative transport properties via the lymphatic and capillary vessels of the two physicochemical states may also contribute to the different pharmacokinetics of these formulations (19). In contrast, the PBS formulation of oct-IP(7)R(26)GLP-1 at room temperature is biologically inactive. Our experiments suggest that under these solution conditions, the formation of this micelle-like form is essentially irreversible and dilution within the subcutaneous space is not sufficient to dissociate this aggregate into readily absorbed units. The conformation(s) of GLP-1 relevant to receptor binding is not known; however, it is noteworthy that oct-IP(7)R(26)GLP-1 represents an example of a peptide that may be administered in two distinctly different secondary structural states, both of which elicit biological responses. Evidently this peptide adopts the biologically active conformation upon post-administration equilibration or alternatively, the population of a unique secondary structural state is not a requirement for receptor signaling.

Effect of Octanoylation on Conformation and Association

The present results show that octanoylation perturbs the conformation of the IP(7)R(26)GLP-1 peptide backbone and alters dramatically its mode of self-association under the higher ionic strength conditions only. In PBS the octanoylated peptide undergoes a major conformational transition involving loss of α-helical structure. The contrasting behavior of the non-acylated peptide shows that the octanoylation confers to the peptide a unique conformational selectivity in response to self-association. Many studies have shown that the insertion of peptides into exogenous micelles, or interaction with organic solvents can significantly alter their secondary structures, usually increasing α-helical content (20–22). Such findings are not surprising given that the exclusion of water is expected to stabilize α-helical structure by enhancing intramolecular hydrogen bonding (23). Indeed, the solution structure of glucagon-like peptide-1(7–36) amide in a dodecylphosphocholine micelle has been determined by NMR to be predominantly α-helical (24). Previous studies have shown that acylation generally causes minor changes in the secondary structure of proteins and peptides although it can increase conformational stability (25–27).

Potential Implications for Intracellular Signaling

Fatty acid acylation is a post-translational modification that occurs in membrane proteins that are involved in intracellular signaling pathways. It is believed that the key function of the acyl group is to act as a hydrophobic anchor to facilitate membrane association and to modulate protein structure for the transmission of biochemical information across the cell membrane (9,28). However, the capacity of acylation to modulate peptide secondary structure has not been definitively established. The present results suggest that the octanoyl acylation confers a propensity for the molecule to undergo an ionic strength-mediated conformational transition to a form that exhibits an unusual temperature-dependent conformational and associative behavior. This finding has possible implications for intracellular signaling pathways as it demonstrates that acylation may influence intermolecular processes and can confer the capacity for a major structural transition triggered by a relatively subtle change in solution conditions.

Subcutaneous Absorption and Bioavailability

The large body of data available for small-molecule drugs establishes that factors such as molecular size, pK_a, solubility, initial drug concentration, injection depth, body movement, blood supply at the injection site and properties of the formulation vehicle can all affect drug release after subcutaneous injection (29). In the case of biopharmaceuticals, the effect of the formulation solution conditions and the subcutaneous environment on secondary and tertiary structure are additional factors. The problem of solid phase aggregate formation in biopharmaceutical preparations has been studied intensively; however, the effects of non-covalent aggregation in the solution phase on absorption and release rates remain relatively unexplored. The major focus of work in this area has dealt with aggregation in protein solutions as it pertains to the physical stability of formulations. The formation of insoluble particulates such as fiber-like particles, translucent particles and gelatinous materials are well-recognized consequences of aggregation that may adversely affect the long-term shelf life of a protein solution and may compromise its compatibility with medical devices (30). Peptides typically exhibit relatively free-ranging backbone conformations with little secondary and/or tertiary structure. Unlike proteins, peptide secondary structure is generally not considered an essential element of their receptor recognition and signaling function. However, the stabilization of the peptide in a particular conformational state may have important consequences for the pharmaceutical properties of the formulated solution. The effect of the physical state of the drug at the site of injection has a well-recognized effect on pharmacokinetics. The administration of solid suspension formulations forms the basis for protracting the time-action of insulin due to the slow dissolution of microcrystals. Formulations administered as emulsions, microspheres and gels also exploit slowed dissolution properties to extend pharmacokinetics (31,32). Subsequent to dissolution, the rate of drug transport from the subcutaneous site to the bloodstream depends primarily upon the permeability of the capillary membrane. The effective size of the transported drug, therefore, is a parameter critical to the

pharmacokinetics of subcutaneous absorption. Consequently, solution conditions that alter the effective size of the drug entity may impact its absorption profile. This principle provides an elegant approach to fine-tuning drug pharmacokinetics. For example, insulin analogs that are more readily dissociated to rapidly absorbed monomers than native insulin produce faster onset pharmacokinetics (33–35). In monomeric insulin analogs the altered self-association properties originate from point mutations. Our study of the oct-IP(7)R(26)GLP-1 molecule demonstrates that factors more subtle than a change in primary structure can affect peptide self-association and subcutaneous absorption.

The conformational and self-association behavior of oct-IP(7)R(26)GLP-1 has been conferred artificially by the introduction of the hydrophobic octanoyl group. However, the present study has wider relevance in demonstrating how peptide hydrophobicity, aggregate size, and the strength of non-covalent interactions in solution formulations can affect the subcutaneous absorption of biopharmaceuticals. When formulated in a low ionic strength diluent the α-helical form is absorbed readily from the subcutaneous site. However, when formulated in PBS at room temperature, the visibly clear, apparently stable solution has little bioavailability after 24 hours. The present results suggest that the therapeutic efficacy of oct-IP(7)R(26)GLP-1 would be seriously compromised were it formulated in a standard clinical isotonic diluent such as a phosphate buffered saline solution at room temperature. In preliminary structure-activity relationship screening studies of biologically active peptides, the formulation diluent serves primarily as a vehicle for drug delivery. The requirements for chemical and physical stability are greatly diminished because shelf-life and in-use stability are minimal compared to those of a marketed peptide solution product. A lyophilized peptide drug candidate may be reconstituted and administered requiring only very short term solution physical and chemical stability for a biopotency assay, animal model experiments, or early phase human clinical trials. The present study shows that when formulating a therapeutic peptide for short term stability, caution must be exercised. Even the seemingly innocuous selection of a widely used "standard physiological diluent" may have a dramatic effect on bioavailability. The potential sensitivity of the peptide to solution conditions indicates a similar caution pertaining to its method of preparation or manufacture. Our study suggests that the utilization of a high ionic strength solvent to solubilize oct-IP(7)R(26)GLP-1 during its manufacture, can result in a lyophilized product that possesses little or no bioavailability upon redissolution. It is concluded that non-covalent aggregation in solution can dramatically influence the bioavailability of a peptide drug, and in the extreme, can totally preclude its absorption, particularly where hydrophobic aggregation mechanisms are involved. This study shows that when oct-IP(7)R(26)GLP-1 is formulated in PBS at 5 °C, it is highly aggregated yet retains substantial bioavailability, suggesting that the critical parameter is the ease of disruption of the intermolecular contacts and thus the strength of the self-association. However, in the case of extremely aggregated peptides and proteins, it is difficult to apply classical biophysical techniques to quantitate the strength of self-association and to correlate such measurements with subcutaneous absorption and transport. The SEC data reported herein show for oct-IP(7)R(26)GLP-1, that this technique distinguishes non-bioavailable peptide aggregate from bioavailable peptide aggregate. This technique may represent a useful general approach for screening solution formulations for soluble non-covalent hydrophobic aggregates of peptides and proteins that are not absorbed subcutaneously.

ACKNOWLEDGMENTS

The authors gratefully acknowledge Eugene Kroeff for providing the peptides, Robert Workman and Judith Heisserman for assistance with the biological studies, and Kingman Ng for assistance with the NONLIN software.

REFERENCES

1. J. L. Cleland and R. Langer in *Formulation and Delivery of Proteins and Peptides*, American Chemical Society, Washington, D.C., 1994, pp 1–19.
2. M. C. Manning, J. E. Matsuura, B. S. Kendrick, J. D. Meyer, J. J. Dormish, M. Vrkljan, J. R. Ruth, J. F. Carpenter, and E. Shefter. *Biotech. Bioeng.* **48**:506–512 (1995).
3. B. Chen, T. Arakawa, C. F. Morris, W. C. Kenny, C. M. Wells, and C. G. Pitt. *Pharm. Res.* **11**:1581–1587 (1994).
4. D. N. Brems. Folding of bovine growth hormone. in *Protein Folding: Deciphering the Second Half of the Genetic Code* (eds. L. M. Gierash and J. King) 129–135, Washington, D. C., 1990).
5. J. London, C. Skrzynia, and M. E. Goldberg. *Eur. J. Biochem.* **47**:409–415 (1974).
6. M. Gutniak, C. Orskov, J. J. Ahren, and B. Efendic. *N. Engl. J. Med.* (1992).
7. M. K. Gutniak, B. Linde, J. J. Holst, and S. Efendic. *Diabetes Care* **17**:1039–1044 (1994).
8. M. Nauck. *Diabetic Medicine* **13**:39–43 (1996).
9. P. J. Casey. *Science* **268**:221–225 (1995).
10. D. Clodfelter, J. Reilly, and M. Nussbaum *submitted for publication.*
11. S. W. Provencher and J. Glockner. *Biochemistry* **20**:33–37 (1981).
12. S. W. Provencher. *CONTIN Users Manual. EMBL Technical Report DA05, European Molecular Biology Laboratory, Heidelberg*, (1982).
13. H. K. Schachman. *Utracentrifugation, Diffusion, and Viscometry*, Academic Press, New York (1957).
14. D. K. McRorie and P. J. Voelker. *Self-Associating Systems in the Analytical Ultracentrifuge*, Beckman Instruments (1993).
15. H. Qi and D. L. Heller. *J. Pharm. Sci. Tech.* **49**:289–293 (1995).
16. Y. Kim and C. A. Rose. *Pharm. Res.* **12**:1284–1288 (1995).
17. W. W. Yau, J. J. Kirkland, and D. D. Bly in *Modern Size Exclusion Chromatography*. Wiley, New York (1979).
18. A. Dong, S. J. Prestrelski, S. D. Allison, and J. F. Carpenter. *J. Pharm. Sci.* **84**:415–424 (1995).
19. Y. Takakura, M. Hashida, and H. Sezaki. Lymphatic transport after parenteral drug administration. In W. N. Charman and V. J. Stella (eds.) *Lymphatic Transport of Drugs* CRC Press, Boca Raton (1992) 255–277.
20. W. Parker and P.-S. Song. *Biophys. J.* **61**:1435–1439 (1992).
21. J. Johansson, G. Nilsson, R. Stromberg, B. Robertson, H. Jornvall, and T. Curstedt. *Biochem. J.* **307**:535–541 (1995).
22. M. M. E. Snel, R. Kapstein, and B. Kruijff. *Biochemistry* **33**:3387 (1991).
23. C. Tanford. *The Hydrophobic Effect*, John Wiley and Sons, New York (1980) 139–145.
24. K. Thornton and D. G. Gorenstein. *Biochemistry* **33**:3532–3539 (1994).
25. W. Yonemoto, M. L. McGlone, and S. S. Taylor. *J. Biol. Chem.* **268**:2348–2352 (1993).
26. K. W. Traxler and T. G. Dewey. *Biochemistry* **33**:1718–1723 (1994).
27. M. Joseph and R. Nagaraj. *J. Biol. Chem* 19439–19445 (1995).
28. G. James and E. N. Olson. *Biochemistry* **29**:2623–2634 (1990).
29. J. Zuidema, F. Kadir, H. A. C. Titulaer, and C. Oussoren. *Int. J. Pharmaceutics* **105**:189–207 (1994).

30. H. R. Constantino, R. Langer, and A. M. Klubanov. *J. Pharm. Sci.* **83**:1662–1669 (1994).
31. J. Heller. Use of Poly(ortho esters) and polyanhydrides in the development of peptide and protein delivery systems. In J. L. Cleland, and R. Langer (eds.) *Formulation and Delivery of Proteins and Peptides*, American Chemical Society, Washington DC (1994) 292–305.
32. Z. Gao, A. J. Shukla, J. R. Johnson, and W. R. Crowley. *Pharm. Res.* **12**:857–863 (1995).
33. J. Brange, U. Ribel, J. F. Hansen, G. Dodson, M. T. Hansen, S. Havelund, S. G. Melberg, F. Norris, K. Norris, L. Snel, A. R. Sorensen, and H. O. Voigt. *Nature* **333**:679–682 (1988).
34. J. Brange, D. R. Owens, S. Kang, and A. Volund. *Diabetes Care* **13**:923–954 (1990).
35. D. L. Bakaysa, J. Radziuk, H. A. Havel, M. L. Brader, S. Li, S. W. Dodd, J. M. Beals, A. H. Pekar, and D. N. Brems. *Protein Science* **5**:2521–2531 (1996).